ResearchGate

See discussions, stats, and author profiles for this publication at: https://www.researchgate.net/publication/231449352

Cyclic voltammetry study of the cation-radical-catalyzed oxygenation of tetraalkyl olefins to dioxetanes

ARTICLE *in* JOURNAL OF THE AMERICAN CHEMICAL SOCIETY · OCTOBER 1986

Impact Factor: 12.11 · DOI: 10.1021/ja00282a004

CITATIONS
30

READS
31

4 AUTHORS, INCLUDING:

Stephen F Nelsen
University of Wisconsin–Madison
118 PUBLICATIONS **2,261** CITATIONS

SEE PROFILE

Available from: Stephen F Nelsen
Retrieved on: 28 January 2016

of the aminoxyl function) and the π orbital of the phenyl ring in these aminoxyls:

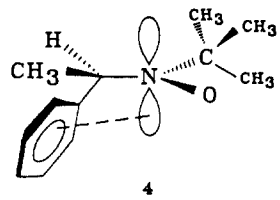

4

The complexing of aromatic molecules with aminoxyls has been reported before, based on a chromatographic experiment.[30] This appears to be the first example of an intramolecular interaction between the aminoxyl function and an aromatic ring. Whether the attraction has electron-transfer character so that the aminoxyl function is reduced or oxidized is not known. An analogous intramolecular orbital interaction (albeit at one bond more distant) has recently been suggested for the carbon centered radical (3-methyl-3-phenylbut-1-yl).[31]

Acknowledgment. This work has been supported by the Natural Sciences and Engineering Research Council of Canada. Continuing support and a grant for the purchase of the ENDOR spectrometer is gratefully acknowledged.

Registry No. XX, 21894-27-9; XXII, 21999-41-7; XXIII, 21572-75-8; PBN, 24293-08-1; PhCH(Et)N(O•)-*t*-Bu, 21984-28-0.

(29) Briere, R.; Chapelet-Letourneux, G.; Lemaire, H.; Rassat, A. *Mol. Phys.* **1971**, *20*, 211.
(30) Batt, L.; Burnett, G. M.; Cameron, G. G.; Cameron, J. *J. Chem. Soc., Chem. Commun.* **1971**, *29*. Burnett, G. M.; Cameron, G. G.; Cameron, J. *J. Chem. Soc., Faraday Trans. 1* **1973**, *69*, 864.
(31) Ingold, K. U.; Nonhebel, D. C.; Wildman, T. A. *J. Phys. Chem.* **1984**, *88*, 1675.

A Cyclic Voltammetry Study of the Cation Radical Catalyzed Oxygenation of Tetraalkyl Olefins to Dioxetanes

Stephen F. Nelsen,* Daniel L. Kapp, Ryoichi Akaba, and Dennis H. Evans

Contribution from the Department of Chemistry, University of Wisconsin, Madison, Wisconsin 53706. *Received January 21, 1986*

Abstract: Cyclic voltammetry studies allow estimation of the rate constant for addition of O_2 to biadamantylidene cation radical ($\mathbf{1}^{\bullet+}$) to be 5600 M^{-1} s^{-1} at room temperature and for the cleavage of biadamantylidene dioxetane cation radical to oxygen and $\mathbf{1}^{\bullet+}$ >800 s^{-1}. Chlorination of the adamantane skeleton slows the overall rate of oxygen addition, and the face selectivity for oxygenation of **5**(Cl) is 25:1 in favor of attack from the olefin face syn to the chlorine. The implications of these findings for the mechanism of the reaction are discussed.

The groups of Nelsen[1] and Clennan[2] simultaneously reported the oxygenation of biadamantylidene (**1**) to its dioxetane **2** by a radical cation chain reaction with ground state. $^3O_2$, which could be initiated by chemical or electrochemical oxidation (Scheme I). Various acidic[3] and oxidizing reagents cause formation of **2**, the epoxide of **1**, and their decomposition products, but it was argued that the cation radical chain mechanism gives essentially only **2**.[1,2] Ando and co-workers[4] have contrasted the stereochemistry of dioxetane formation for analogues of **1** in the electrochemically initiated reaction with those of photogenerated $^1O_2$ and by photolysis with reducible sensitizers like 9,10-dicyanoanthracene, which initially generates pairs of olefin cations and O_2^{-}.[5] The use of $\mathbf{3}^{\bullet+}$,[6] a powerful enough oxidant to form tetraalkylolefin cation radicals rapidly at low temperature, makes the cation radical chain oxygenation reaction preparatively useful.[7] Conversion of isopropylideneadamantane (**4**) to dioxetane under

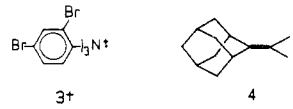

3+ 4

these conditions without formation of the allylic hydroperoxide, which is the sole product both with $^1O_2$ and easily reduced photosensitizers, showed that the chemistry of the cation radical chain oxygenation reaction is effectively separate from that of the other reaction conditions.[7] Dioxetane cation radicals have been demonstrated to build up at −78 °C in the absence of reductants,[8] and the oxidation of **1** by $\mathbf{2}^{\bullet+}$ has been shown to be quite exothermic at −78 °C, providing the driving force for an effective chain reaction. MNDO-level calculations[9] suggest that oxygen adds to olefin cations one C–O bond at a time, and evidence for C–C bond rotation of an open O_2, olefin cation radical adduct, has been provided by product studies on an analogue of **1**.[10]

Scheme I

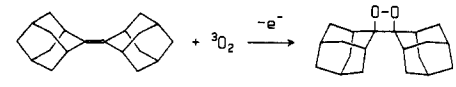

1 2

This paper gives a full report on the contribution of cyclic voltammetry (CV) studies to the elucidation of the mechanism of cation radical chain oxygenation of monoolefins of dioxetanes, including an investigation of the effect of heteroatom substituents on **1** on both electron loss and oxygen addition.

Results

One-Electron Oxidation of 1 Analogues. **1** gives chemically reversible CV curves at 0.05 V/s in acetonitrile (0.1 M in *n*-Bu_4NClO_4, $E^{\circ\prime}$ 1.44 V vs. SCE[11]) and methylene chloride (0.1 M in *n*-Bu_4NClO_4, $E^{\circ\prime}$ 1.53 V[1]), showing that $\mathbf{1}^{\bullet+}$ lasts at least

(1) Nelsen, S. F.; Akaba, R. *J. Am. Chem. Soc.* **1981**, *103*, 2096.
(2) Clennan, E. L.; Simmons, W.; Almgren, C. W. *J. Am. Chem. Soc.* **1981**, *103*, 2098.
(3) Akaba, R.; Sakuragi, H.; Tokumaru, K. *Tetrahedron Lett.* **1984**, *25*, 665.
(4) (a) Ando, W.; Kabe, Y.; Takata, T. *J. Am. Chem. Soc.* **1982**, *104*, 7314. (b) Kabe, Y.; Takata, T.; Ueno, K.; Ando, W. *Ibid.* **1984**, *106*, 8174.
(5) Schaap, A. P.; Zaklika, K. A.; Kaskar, B.; Fung, L. W.-M. *J. Am. Chem. Soc.* **1980**, *102*, 389.
(6) Schmidt, W.; Steckhan, E. *Chem. Ber.* **1980**, *113*, 577.
(7) Nelsen, S. F.; Kapp, D. L.; Teasley, M. F. *J. Org. Chem.* **1984**, *49*, 579.
(8) Nelsen, S. F.; Kapp, D. L.; Gerson, F.; Lopez, J. *J. Am. Chem. Soc.* **1986**, *108*, 1027.
(9) Chen, C.-C.; Fox, M. A. *J. Comput. Chem.* **1983**, *4*, 488.
(10) Nelsen, S. F.; Kapp, D. L. *J. Am. Chem. Soc.* **1986**, *108*, 1265.
(11) Nelsen, S. F.; Kessel, C. R. *J. Am. Chem. Soc.* **1979**, *101*, 2503.

0002-7863/86/1508-6863$01.50/0 © 1986 American Chemical Society

Table I. Oxidation Potentials for Substituted Biadamantylidines[a]

compd	23 °C $E°'[\Delta E_{pp}]$[b]	−78 °C $E°'[\Delta E_{pp}]$
1	1.62 [0.06]	1.59 [0.10]
5 (OMe)	solvolyzes	1.77 [0.23]
5 (Cl)	solvolyzes	1.78 [0.12]
5 (O_2CF_3)	1.87 [0.075]	1.82 [0.11]
6 (OMe)	1.86 [0.075]	1.82 [0.165]
7 (Cl_2)	2.02 [0.08]	1.99 [0.14]

1 s in these solvents in the absence of oxygen. Subsequent experiments have shown that its lifetime is not much longer than seconds in these solvents, however. For example, addition of $\mathbf{3}^{\bullet+}$ $SbCl_6^-$ ($E°'$ 1.60 in CH_2Cl_2/0.1 M n-Bu_4NClO_4) generates the purple color[12] of $\mathbf{1}^{\bullet+}$, but this color fades within several seconds; a principal product isolated from these solutions is 4(e)-chloroadamantylideneadamantane, **5**(Cl). Cyclic voltammograms in these solvents show a second, irreversible oxidation wave only slightly positive of the $\mathbf{1},\mathbf{1}^{\bullet+}$ couple, peaking at 1.87 V at a 0.2 V/s scan rate in CH_2Cl_2/0.1 M n-Bu_4NClO_4. The decomposition appears to produce acid, since scanning back to low potentials after scanning up into this wave at a platinum electrode gives a distended chemically reversible wave corresponding to reduction of protons (centered at +0.35 V in CH_2Cl_2/0.1 M n-Bu_4NClO_4). We suggest that disproportionation of $\mathbf{1}^{\bullet+}$ is likely to be involved in its rather rapid decomposition and that the dication formation is coupled with deprotonation. Hammerich and Parker[13] showed that addition of acids to arene solutions greatly extended the lifetimes of the cation radicals, presumably by removing traces of water and other basic impurities. Addition of 5% (volume/volume) each of trifluoroacetic acid and trifluoroacetic anhydride to a CH_2Cl_2 solution which is 0.1 M in supporting electrolyte (which we will subsequently refer to as a 20:1:1 solvent mixture, and which was used throughout this work as a CV solvent) shifts the irreversible second wave to more positive potentials, as expected if the second wave is coupled to very rapid deprotonation of $\mathbf{1}^{2+}$; the reversible first electron-transfer wave doses not shift. **1** proved to be consumed over a period of many minutes when n-Bu_4NClO_4 was used as the supporting electrolyte in the 20:1:1 solvent mixture. This is presumably caused by its reaction with perchloric acid generated under these conditions, because switching the supporting electrolyte to n-Bu_4NBF_4 alleviates this problem, and the tetrafluoroborate supporting electrolyte was used for all cv experiments reported below.

To study the effect of electron-withdrawing groups on the ease of oxidation, some heteroatom substituted derivatives of **1** were examined. Wynberg and co-workers[14] showed that treatment of **1** with positive halogen sources gives 4(e)-substituted derivatives, and we made the 4(e)-Cl derivative **5**(Cl) by using N-chlorosuccinimide. They also reported[15] that silver nitrate in aqueous THF converts **5**(Cl) to **5**(OH). We found that silver nitrate in

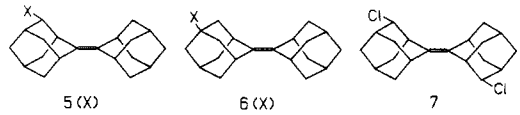

5 (X) 6 (X) 7

methanolic THF gave a 1:2 mixture of **5**(OMe) and **5**(ONO_2). Somewhat surprisingly to us, **5**(Cl) was found to solvolyze in CF_3CO_2H,CH_2Cl_2 at room temperature to give **5**(O_2CCF_3). **6**(OMe) was prepared by O-methylation of 5-hydroxy-2-adamantanone,[16] addition of 2-adamantyllithium, and dehydration. The diequatorial dichloro compound was made by the published method;[14] the chlorines have been argued to be in separate adamantane rings, but the sites of substitution in one adamantane relative to the other are not known.

(12) Nelsen, S. F.; Teasley, M. F.; Kapp, D. L.; Kessel, C R.; Grezzo, L. A. *J. Am. Chem. Soc.* **1984**, *106*, 791.
(13) Hammerich, O.; Parker, V. D. *Electrochim. Acta* **1973**, *18*, 537.
(14) Meijer, E. W.; Kellog, R. M.; Wynberg, H. *J. Org. Chem.* **1982**, *47*, 2005 and references therein.
(15) Wieringa, J. H.; Strating, J.; Wynberg, H. *Tetrahedron Lett.* **1970**, 4579.
(16) Geluk, H. W.; Schlatmann, J. L. M. A. *Tetrahedron* **1968**, *24*, 5369.

Table II. Oxidation Potentials for Some Tetraalkyl Olefins[a]

structure	compd	23 °C $E°'[\Delta E_{pp}]$[b]	−78 °C $E°'[\Delta E_{pp}]$
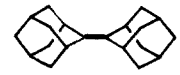	**1**	1.62 [0.06_0]	1.59 [0.10_0]
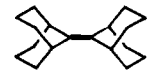	**8**	1.67 [0.07_8]	1.63 [0.09_3]
	**9**	1.73 [0.07_5]	1.68 [0.17][c]
	**10**	1.72 [0.07_5]	1.67 [0.12][c]
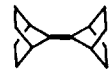	**11**	irrev[d]	2.04 [0.10][c]
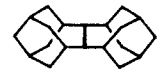	**12**	1.52 [0.08_4]	1.47 [0.09_4]
	**13**	1.68 [0.06_5][c]	1.64 [0.07_0][c]
	**14**	1.61 [0.08_9][c]	1.56 [0.08_8][c]
	**15**	1.43 [0.08_0][c]	1.40 [0.10_1][c]
	**16**	1.92 [0.11][f]	1.88 [0.14]
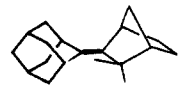	**17**	1.66 [0.08_2]	1.61 [0.12]
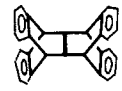	**18**	1.61 [0.10]	1.62 [0.10]
	**19**	1.78 [0.17][e]	1.70 [0.20]
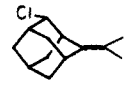	**20**	1.93 [0.10][e]	1.89 [0.12]
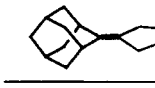	**21**	1.74 [0.07_8]	1.70 [0.08_1]

Table I shows the $E°'$ values measured at room temperature and −78 °C for these compounds, although both **5**(Cl) and **5**(OMe) solvolyzed too rapidly at room temperature in the 20:1:1 solvent used to obtain room temperature data.

The oxidation of several other tetraalkylolefins has also been studied by CV under the same conditions as the compounds of Table I, and these data appear in Table II. The compounds containing methyl groups on the C=C bonds, **19** and **20**, gave cation radicals which were much shorter-lived than the others and only showed a reduction wave at fast scan rates at room temperature, but the diethyl substituted compound **21** gave a noticeably longer-lived cation radical.

Results and Discussion

Quantitative Study of 1, $^3O_2$ Cyclic Voltammograms. The cyclic voltammetry curves for **1** in an oxygen saturated solution show the characteristic wave shapes for EC backwards E (ECbE) electrochemistry, first studied in detail by Feldberg and Jeftic[17]

(17) Feldberg, S. W.; Jeftic, L. *J. Phys. Chem.* **1972**, *76*, 2439.

for the reduction of chromium(III) hexacyanide complexes. Recently, Kochi's group has studied electrocatalyzed ligand substitution in a series of manganese complexes by using cyclic voltammetry simulations,[18,19] obtaining good fit to a four-step ECbE kinetic scheme.

Our initial attempts at quantitatively simulating the cv curves observed for oxidation of **1** were largely frustrated by the presence of the irreversible $\mathbf{1}^+,\mathbf{1}^{2+}$ wave so close to the $\mathbf{1},\mathbf{1}^+$ wave, which caused distortion of the observed curves. Use of the 20:1:1 solvent system shifts the irreversible wave to substantially more positive potential, allowing a more quantitative treatment of the data. The digital simulation method of Feldberg[20] was used to generate the theoretical cyclic voltammograms.[21] The results obtained for **1** in the absence of oxygen in 20:1:1 solvent at room temperature could be accounted for by a simple one-electron quasireversible oxidation. An example is shown in Figure 1, where the digitized experimental data (circles) and simulated cyclic voltammogram (line) are compared for a scan rate of 0.5 V/s. A value of $k_s/D^{1/2}$ of 16 $s^{-1/2}$ (where k_s is the standard heterogeneous electron transfer rate constant and D is the diffusion coefficient) produces the 0.072 V peak separation seen in the experiment. An electron-transfer coefficient, α, of 0.5 was used. The peak separation in the experimental voltammogram is close to the reversible limit of 0.057 V at 24 °C, and the deviation can be due in part to residual uncompensated resistance. Therefore, no quantitative significance should be imparted to the value of k_s reported above. However, it was found that $k_s/D^{1/2} = 16$ $s^{-1/2}$ also produced a simulated voltammogram in good agreement with the 0.05 V/s data.

It can be seen in Figure 1 that the observed current at positive potentials near the switching potential exceeds the simulated level. This tendency, which is common to all of our data, is even more pronounced in CH_2Cl_2 solvent. The use of the 20:1:1 solvent greatly alleviated this discrepancy but did not completely eliminate it.

When **1** is oxidized in the presence of oxygen, the voltammograms exhibit the characteristics of ECbE process, viz., the anodic peak current is very small and a zero current crossing is seen on the positive-going scan at slow scan rates.[1] The simplest kinetic scheme which could fit the data is shown in Scheme II. Oxidation

Scheme II

$$\mathbf{1} \rightleftarrows e^- + \mathbf{1}^+ \qquad E^{\circ\prime} = 1.62 \text{ V} \qquad \text{(step 1)}$$

$$O_2 + \mathbf{1}^+ \xrightarrow{k_{on}} \mathbf{2}^+ \qquad \text{(step 2)}$$

$$e^- + \mathbf{2}^+ \rightleftarrows \mathbf{2} \qquad E^{\circ\prime} = 2.29 \text{ V} \qquad \text{(step 3)}$$

$$\mathbf{1} + \mathbf{2}^+ \xrightarrow{k_{et}} \mathbf{1}^+ + \mathbf{2} \qquad \text{(step 4)}$$

$$\mathbf{2}^+ \xrightarrow{k_{dec}} \text{products} \qquad \text{(step 5)}$$

of **1** occurs in step 1 followed by addition of oxygen to the olefin cation to give the dioxetane cation with a rate constant, k_{on}. Steps 3–5 provide for the disappearance of the dioxetane cation. $E^{\circ\prime}$ for $\mathbf{2},\mathbf{2}^+$ is about +2.25 V at −78 °C, and its value will be higher at room temperature (see the room temperature and −78 °C data in Tables I and II; we used +2.29 V in the simulations). The 0.67 V (15.4 kcal/mol) exothermicity for step 4 is certainly expected to make k_{et} close to the diffusion-controlled limit. Simulations were found to be independent of k_{et} as long as it exceeded about 10^6 L mol^{-1} s^{-1} so we used a diffusion-controlled rate in the simulations. Similarly, the most positive potentials in the voltammograms are over 0.4 V negative of $E^{\circ\prime}$ for $\mathbf{2},\mathbf{2}^+$ causing step 3 to be very rapid so the surface concentration of $\mathbf{2}^+$ was maintained at zero in the simulations.

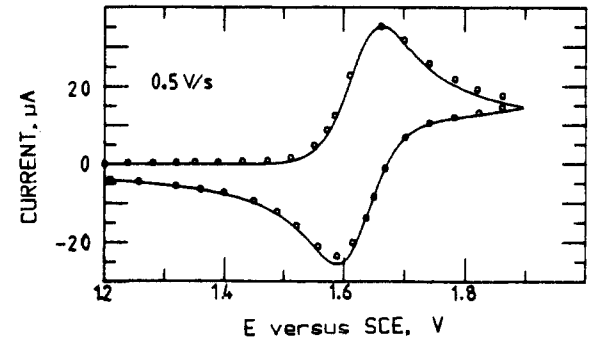

Figure 1. CV of biadamantylidene, **1**, at 24 °C under a nitrogen atmosphere; circles: obsd, line: calcd.

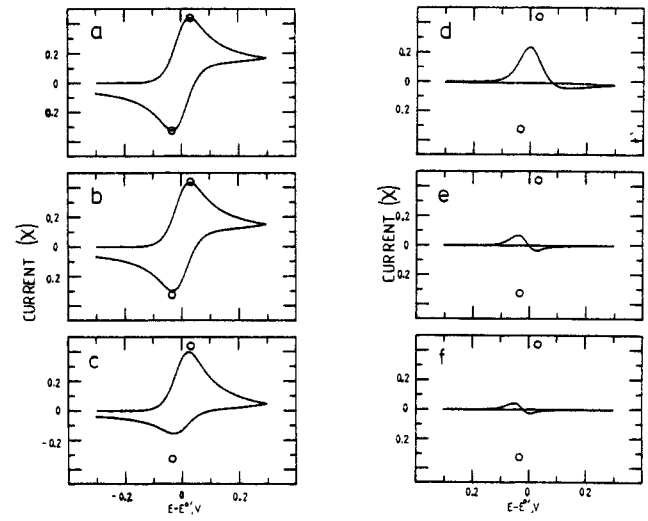

Figure 2. Changes in peak shape for ECbE electron transfer (Scheme III, steps 1–4) as k_{on} is increased. Simulation is at 2 mM [**1**] 7.5 mM [O_2], SCANP = 0.1, at k_{on} values (M^{-1} s^{-1}) a; 1; b, 10; c, 10^2; d, 10^3; e, 10^4; f, 10^5; all for a scan rate of 0.2 V/s. The circles designate the coordinates of the anodic and cathodic peaks under the same conditions in the absence of oxygen.

Table III. Conditions for CV Experiments on Oxidation of **1** in the Presence of O_2

data set	[**1**], mM	atmosphere
A	2.24	air
B	1.09	O_2
C	2.68	O_2

To illustrate the voltammetric behavior expected for the ECbE scheme under our typical experimental conditions, a series of voltammograms was simulated (Figure 2) in which step 5, Scheme II, was omitted ($k_{dec} = 0$). In this series the scan rate is held constant (0.2 V/s), and k_{on} is increased from $1–10^5$ L mol^{-1} s^{-1}. The circles on the plots denote the coordinates of the anodic and cathodic peaks in the absence of oxygen to aid in judging the effects of oxygen on the voltammetric response. As k_{on} increases, the first effect observed is a smaller reduction current on the return sweep, but then the oxidation peak current diminishes, and the peak shifts to less positive potentials. The current positive of E_p^{ox} begins to decrease considerably faster than the $t^{-1/2}$ dependence observed for a diffusion-controlled electrode reaction uncomplicated by coupled chemical reactions. Negative currents are eventually obtained near $E^{\circ\prime}$ of $\mathbf{1},\mathbf{1}^+$ when k_{on} is large. At still higher values of k_{on}, almost no current is observed throughout the range of potential scanned. This happens when the rates of steps 1–4 become so large that only the overall reaction of **1** with O_2 giving **2** occurs with almost no charge being passed through the cell.

(18) Hershberger, J. W.; Klinger, R. J.; Kochi, J. K. *J. Am. Chem. Soc.* **1983**, *105*, 61.
(19) Zizelman, P. M.; Amatore, C.; Kochi, J. K. *J. Am. Chem. Soc.* **1984**, *106*, 3371.
(20) Feldberg, S. W. In *Electroanalytical Chemistry*; Bard, A. J., Ed.; Marcel Dekker: New York, 1969; Vol. 3, p 199. See, also: Feldberg, W. W. In *Computer Application in Analytical Chemsitry*; Mark, H. B., Ed.; Marcel Dekker: New York, 1972; Vol. 2, Chapter 7.
(21) Full details, including a listing of the simulation programs used, appear in the Ph.D. Thesis of Kapp, D. L., University of Wisconsin, Madison, 1985.

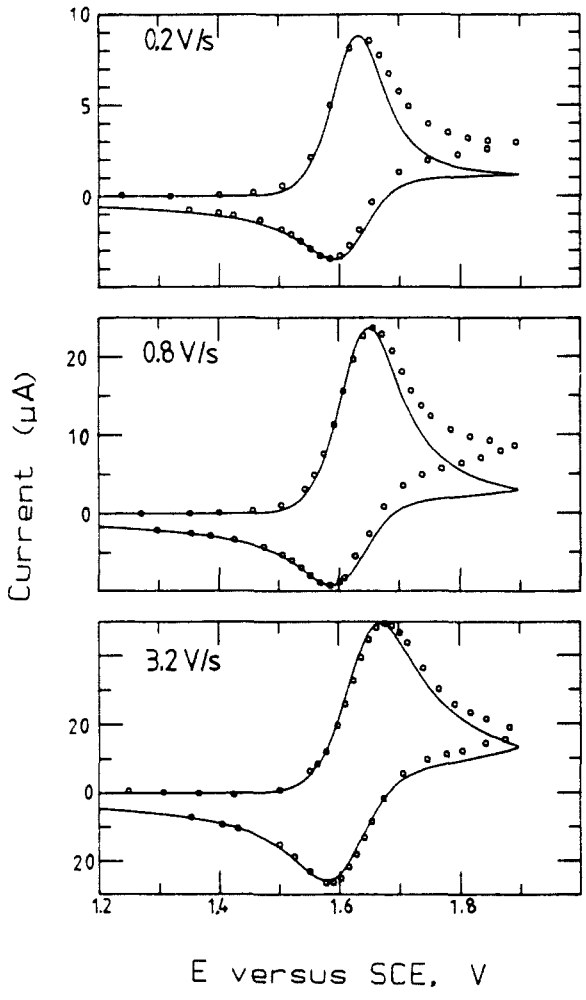

Figure 3. CV curves for 2.24 mM **1** under air (1.65 mM O^2) at 21 °C (data set A) at the scan rates shown on the plots.

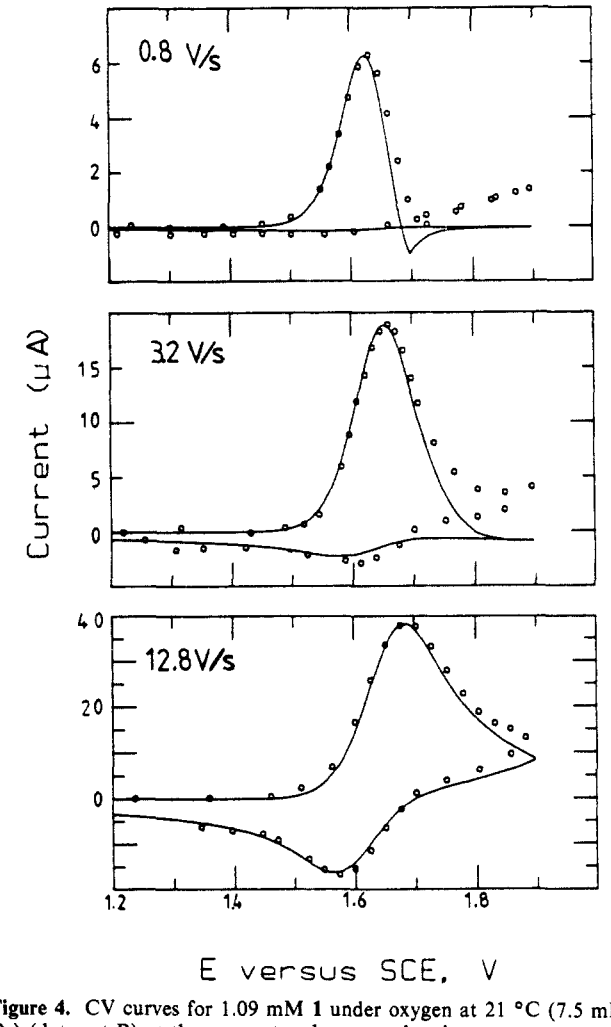

Figure 4. CV curves for 1.09 mM **1** under oxygen at 21 °C (7.5 mM O_2) (data set B) at the scan rates shown on the plots.

Although we were able to fit the oxidation scans reasonably by using steps 1–4 of Scheme II, the calculated reduction currents were always far higher than those observed. This behavior is attributed to the instability of the dioxetane radical cation $\mathbf{2}^+$, which decomposes rapidly on the CV time scale at room temperature. Study of **2** oxidation (see below) showed that k_{dec} exceeds 800 s^{-1} under these conditions which is fast on the time scale of these experiments. Inclusion of step 5 allowed reasonable simulation of the experimental data.

Quantitative voltammograms were obtianed under three sets of conditions at 21 °C, shown in Table III. The experimental data are shown as circles in Figures 3–5, with simulations of the voltammograms shown as lines. The simulated and observed currents have been made qualitatively at the anodic peak. Comparisons of set A and C show that the data are quite sensitive to the concentration of oxygen in the solution. The solubility of O_2 in our solvent mixture has not been measured in the literature, nor has it even been measured in pure methylene chloride. The organic solvents reported have O_2 solubilities varying from 4 to 12 mM at room temperature,[23] and the solubilities for CCl_4 and $CHCl_4$ have been reported to be 12 and 10 mM, respectively.[24] The data for set A are especially sensitive to $[O_2]$, because the oxygen and olefin concentrations are comparable, and oxygen depletion effects occur at slow scan rates. All three data sets are fit best by using $[O_2]$ = 7.5 mM in a pure O_2 atmosphere, (0.21)(7.5) = 1.58 mM for air-saturated, and k_{on} = 5600 M^{-1} s^{-1}. There is little effect on the shape of the O_2-saturated simulation sets B and C when k_{on} and $[O_2]$ are varied while the pseudo-first-order term $k_{on}[O_2]$ is kept constant at 42 s^{-1}, but the oxidation-to-reduction current ratio is quite sensitive for set A, where the $[O_2]$ is lower. By examining the effects of varying both quantities on the simulations, we estimate that our best value of $k_{on}[O_2]$ is accurate to 10%. We also compared the relative values of the anodic peak current as a function of scan rate with the simulated peak current functions. For the ECbE mechanism, the peak current function is very dependent upon scan rate, its predicted value varying over a factor of two for the range of conditions in data sets A, B, and C. The observed peak currents tracked the predicted dependence on scan rate within 15% for all the data, an observation which supports the adequacy of Scheme II to account for the data.

CV of 2. The above simulations were carried out with the simplest kinetic scheme which would fit the data, but as indicated in the introduction, the mechanism for O_2 addition to $\mathbf{1}^+$ is almost certainly a two-step addition, and as will be shown below, when $\mathbf{2}^+$ decomposes, it generates some $\mathbf{1}^+$, so both steps must be reversible. We have carried out some studies on the $\mathbf{2},\mathbf{2}^+$ electron transfer to help consider the effects which other reactions going on in the solution have on the interpretation of the k_{on} value obtained above. Although $\mathbf{2}^+$ is stable enough at −78 °C to give approximately chemically reversible CV curves, a very large peak-to-peak separation (indicating slow heterogeneous electron transfer) was observed; we found[8] ΔE_{pp} = 0.15 V and $E^{\circ\prime}$ = 2.25 at 0.2 V/s scan rate, and ΔE_{pp} = 0.22 V and $E^{\circ\prime}$ = 2.27 at 2.0 V/s scan rate (The latter value of $E^{\circ\prime}$ is probably the less reliable because of the larger peak separation). What we had not realized at the time of our earlier publication[8] is that the observed peak-to-peak separation (but not $E^{\circ\prime}$) is extremely sensitive to electrode

(22) *Electroanalytical Methods*; Bard, A. J., Faulkner, L. R., Eds.; J. Wiley and Sons: New York, 1980; Chapter 3.
(23) Achord, J. M.; Hussey, C. L. *Anal. Chem.* **1980**, *52*, 512.
(24) Batlino, R.; Retlich, T. R.; Tominaga, T. *J. Phys. Chem. Ref. Data* **1982**, *12*, 163.

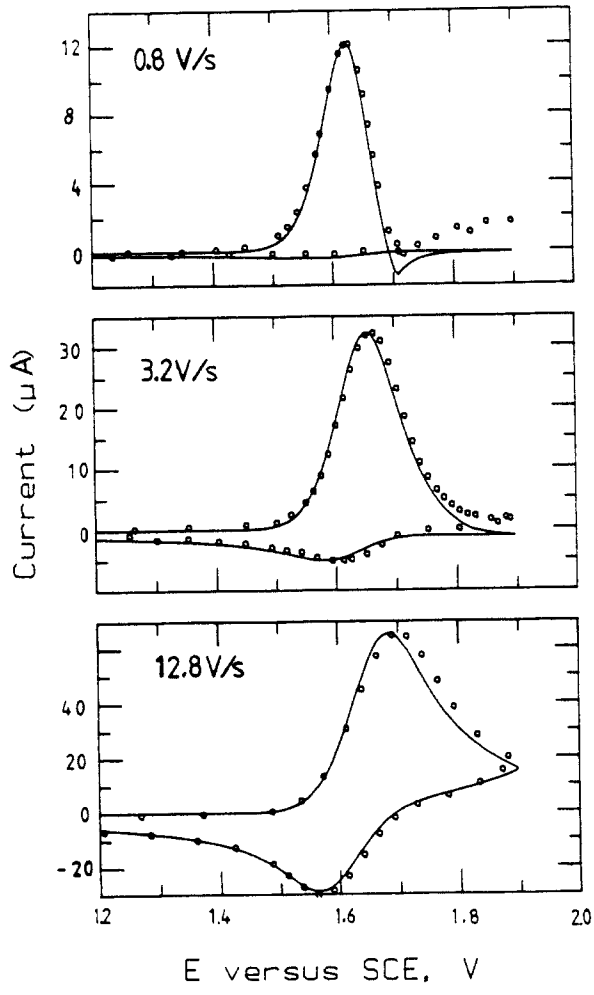

Figure 5. CV curves for 2.68 mM **1** under oxygen at 21 °C (7.5 mM O_2) (data set B) at the scan rates shown on the plots.

conditions and that as time passed, we observed increasingly larger separations, even after extensive cleaning and repolishing of the electrodes.

At room temperature the CV wave for $\mathbf{2,2}^+$ remains totally irreversible (no reduction wave detected) at a scan rate of 50 V/s. Simulations showed that k_{dec} of $\mathbf{2}^+$ must be at least 800 s^{-1} to fit this observation. Decompostion of $\mathbf{2}^+$ at room temperature under nitrogen saturation is accompanied by formation of $\mathbf{1}^+$. We had missed this fact in our earlier CV work[8] because the $\mathbf{1}^+$ reduction wave observed is rather small compared to the **2** oxidation wave, and because the $\mathbf{1}^+$ reduction wave can only be observed at faster scan rates. We had initially not appreciated that diffusion is slow enough that the $[O_2]$ near the $\mathbf{1}^+$ formed remains high, and readdition competes favorably with diffusion at low scan rates, making the reduction wave for $\mathbf{1}^+$ vanishingly small. A somewhat similar kinetic situation was encountered in the dimerization of phenoxy radicals generated by oxidation of phenolates.[25] Figure 6 shows the CV curve observed for **2** at room temperature under nitrogen for a scan that includes the region for $\mathbf{1}^+$ reduction on the return scan, at a scan rate of 0.8 V/s. This curve was simulated by using Scheme III and as usual, the simulation is displayed as the line in Figure 6. The size of the $\mathbf{1}^+$ reduction wave is calculated to depend on the relative rates of k_{dec} and k_{off}. We gradually increased k_{dec} until the reduction wave was the correct size relative to the oxidation wave and found adequate fit (that shown in Figure 6) when $k_{off} = k_{dec} > 800$ s^{-1}. These simulations ignored $\mathbf{1}^+$ oxidation, which we know occurs in the region where dioxetane oxidizes but cannot fit adequately because the process is completely irreversible, and we have no way of knowing what the heterogeneous rate of the reaction actually is, so the k_{dec} value of 800 s^{-1} is a minimum value. Inclusion of the k_{off} process ($\mathbf{2}^+ \rightarrow \mathbf{1}^+ + O_2$) with a value of $k_{off} = 800$ s^{-1} has no effect on the simulations of olefin oxidation when oxygen is present because electron transfer of dioxetane cation radical with neutral olefin was estimated to have a very large k_{et} value; it is quite exothermic, and the k_{off} process does not compete by using $k_{et} > 10^6$ L mol^{-1} s^{-1}; we employed diffusion-controlled electron transfer.

Scheme III

$$\mathbf{2} \rightarrow e^- + \mathbf{2}^+ \qquad E^{\circ\prime} = 2.29 \text{ V} \qquad \text{(step 1)}$$

$$\mathbf{2}^+ \underset{k_{on}}{\overset{k_{off}}{\rightleftharpoons}} \mathbf{1}^+ + O_2 \qquad \text{(step 2)}$$

$$\mathbf{2}^+ \xrightarrow{k_{dec}} \text{products} \qquad \text{(step 3)}$$

$$e^- + \mathbf{1}^+ \rightarrow \mathbf{1} \qquad E^{\circ\prime} = 1.62 \text{ V} \qquad \text{(step 4)}$$

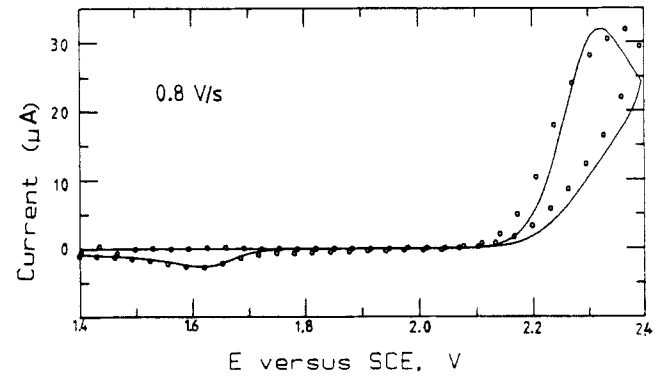

Figure 6. CV curve for biadamantylidene dioxetane **2** at room temperature under nitrogen, showing the irreversible oxidation wave for $\mathbf{2,2}^+$ and the small reduction wave for $\mathbf{1}^+$,**1** near 1.6 V.

Relative Oxygen Addition Rates at −78 °C. To examine the relative reactivities of various olefin cation radicals with oxygen, we have chosen to compare their CV curves in the olefin cation oxidation region at −78 °C at a scan rate of 0.5 V/s, because both the olefin radical cations and the dioxetane radical cations are long-lived on the CV time scale under these conditions. Steric hindrance is obviously important in determining the rate of oxygen addition. Isopropylideneadamantane, **20**, shows only a tiny oxidation wave under these conditions,[7] and its k_{on} value is too large to estimate quantitatively relative to the other compounds. At the other end of the reactivity scale, the more sterically hindered of the Bredt's rule protected[11] compounds, **12** and **13**, which have their bicyclic groups attached 1,2 on the C=C bond ("sesquibicyclic" using the nomenclature introduced by Bartlett and co-workers[26]) show no effect on their CV curves when a nitrogen atmosphere is replaced by an oxygen atmosphere, so k_{on} is clearly too small to estimate the rates of reaction of their radical cations with oxygen under these conditions. No effect of oxygen was observed on the CV curve of **17**, which has one tertiary alkyl group attached to the olefin, apparently because the steric effect is still large enough to make k_{on} quite small. Although the sesquinorbornenes **14** and **15** show CV curves that are affected by oxygen, they do not show ECbE behavior and do not give significant yields of dioxetanes. They are clearly undergoing different sorts of reactions than the dialkylidenes and will not be further discussed here. Figure 7 shows the CV curves for the compounds which do have k_{on} values in the rate range that affects the CV curves at −78 °C. From the appearance of these curves, the reactivity order is clearly **1** > **5**(Cl) > **7**(Cl_2) > **9** ~ **10** (compare with Figure 2). More quantitative estimation of the relative rates was attempted by simulation. Unfortunately, the agreement between simulation (the lines in Figure 7) and experiment was not good for some of the compounds. We do not know the source of the discrepancy. The kinetic parameter $k_{on}[O_2]$ was adjusted to give what was deemed to be best fit to the experimental data

(25) Evans, D. H.; Jimenez, P. J.; Kelly, M. J. *J. Electroanal. Chem.* **1984**, *163*, 145.

(26) Bartlett, P. D.; Blakeney, A. J.; Kimura, M.; Watson, W. H. *J. Am. Chem. Soc.* **1980**, *102*, 1383.

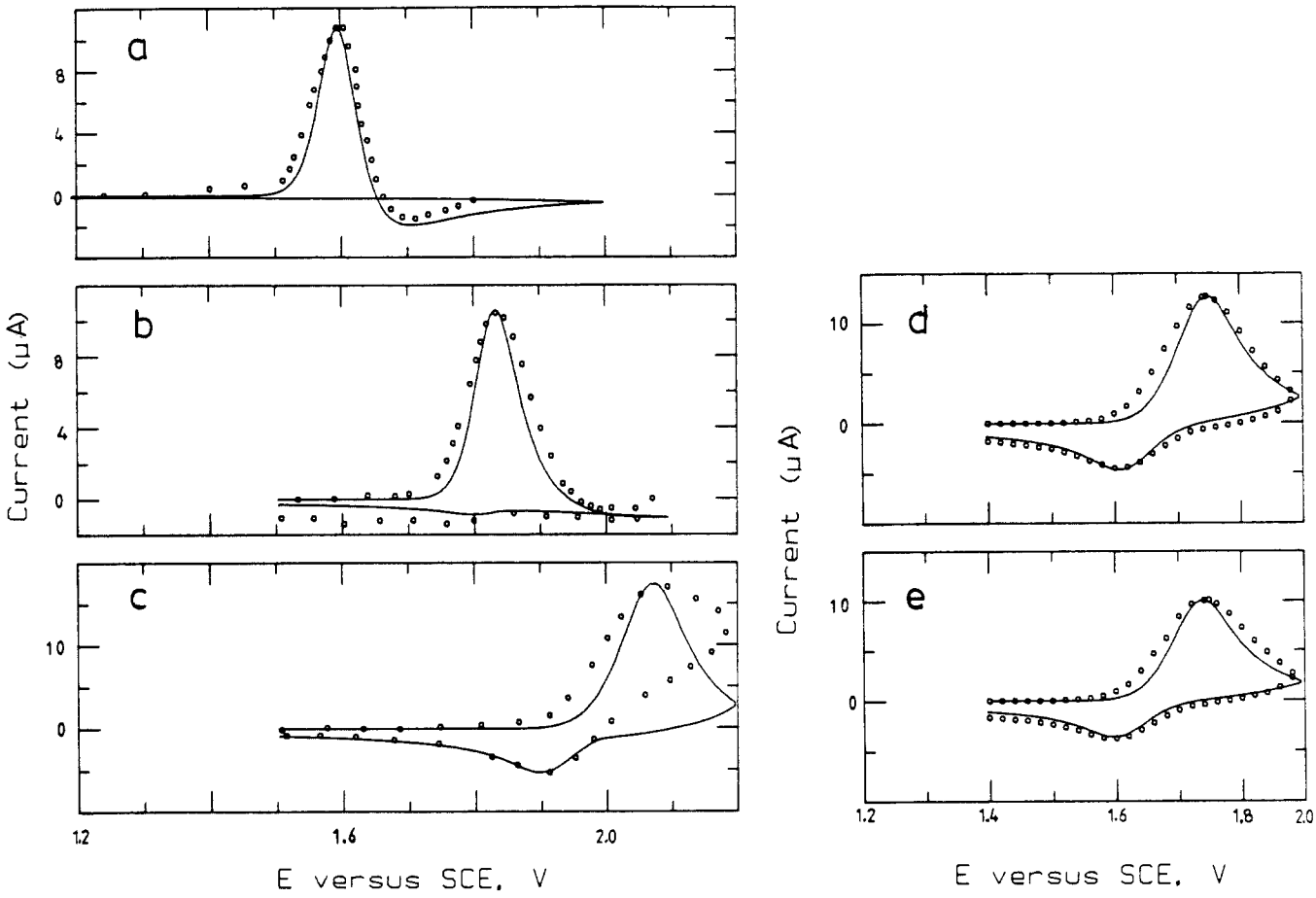

Figure 7. (a–c) CV curves for **1**, **5**(Cl), and **7**(C12), respectively, at −78 °C under oxygen at 0.5 V/s scan rates. (d–e) CV curves for **9** and **10** at −78 °C under oxygen at 0.5 V/s scan rates.

Table IV. Relative Rate Constants for O_2 Addition to Some Olefin Radical Cations at −78 °C

olefin	$k_{on}[O_2]$, s^{-1} mM	relative k_{on}
1	22500	7.5
5(Cl)	9000	3
7(C12)	4500	1.5
9	3000	1
10	3000	1

(the criteria used were ratio of oxidation to reduction peak currents and location of peak maxima).

Selectivity for Dioxetane Formation from 5(Cl). The reaction of $^1O_2$ with **5**(Cl) was reported by Wynberg and co-workers[27] to give an excess of the syn dioxetane **22** over **23**, although the experimental details and ratios have not been given. We observed a 3.1:1 ratio of **22**:**23** when **5**(Cl) was irradiated under oxygen with tetraphenylporphyrin as photosensitizier ($^1O_2$ conditions), see Scheme IV. Our assignments are based on the literature assignments[28] of the reduction products of **24** with borohydrides, **25** and **26**, which are based on pseudocontact shifts, and on the isopropyllithium adducts **27** and **28** (see Experimental Section).

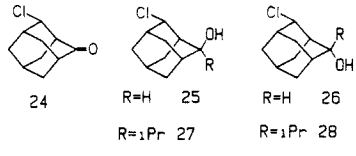

Only **22**, the major isomer in the $^1O_2$ reaction, was obtained from **5**(Cl) upon radical chain photooxygenation at −78 °C after one crystallization from methanol, but the NMR spectrum of the crude reaction product showed the presence of some of the minor isomer, and NMR integration gave a 25:1 ratio of **22**:**23**. Dioxetane formation under the olefin radical cation chain conditions favors the same product, that of addition from the same side of the olefin as the chlorine substituent, but the selectivity is somewhat higher: 25:1 at −78 °C corresponds to a ΔG^* difference of 1.2 kcal/mol, while 3.1 at 25 °C corresponds to 0.7 kcal/mol.

Scheme IV

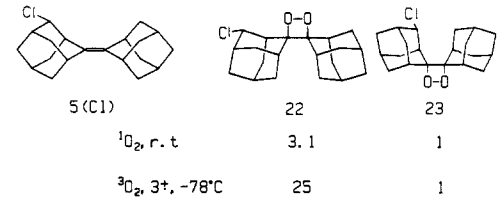

Oxidation Potentials of Tetraalkylolefins. It can be noted from Table I that heteroatom substitution at C(4) (β to the vinyl carbon) and C(5) (γ to the vinyl carbon) causes significant destabilization of the cation radical relative to the neutral olefin. Comparison of the $E°'$(−78 °C) values gives thermodynamic destabilizations of 4.3 kcal/mol for 4-OMe and -Cl substitution, 5.3 kcal/mol for 5-OMe and 4-O_2CCF_3 substitution, and 9.2 kcal/mol for 4,4′-Cl_2 substitution relative to the $\mathbf{1,1}^+$ couple. The slightly larger effect for 5-OMe than 4-OMe substitution indicates that the effect is not simply through-space destabilization by the C–X dipole. Unusually large σ,π interaction in $\mathbf{1}^+$ is indicated both by its ESR[29] and optical[12] spectra. The larger ESR splitting constant observed for the hydrogen at C(5) than H_{eq} at C(4) is consistent with the greater effect on $E°'$, and we suggest that there

(27) (a) Wynberg, H.; Meijer, E. W.; Hummelen, J. C. *Bioluminescence and Chemiluminescence*; Deluca, M. A., McElroy, W. D., Eds.; Academic Press: New York, 1981; p 687. (b) Hummelen, J. C.; Meijer, E. W.; Wynberg, H. *Chem. Abstr.* **1984**, *100*, 209242h (PTC Int. Appl. WO 83 03 604).
(28) Giddings, M. R.; Huduc, J. *Can. J. Chem.* **1981**, *59*, 459.
(29) Gerson, F.; Lopez, J.; Akaba, R.; Nelsen, S. F. *J. Am. Chem. Soc.* **1981**, *103*, 6716.

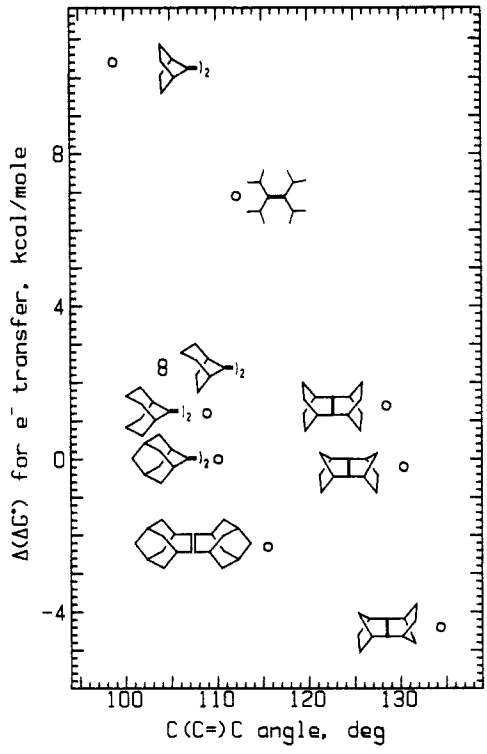

Figure 8. Plot for changes in ΔG for electron transfer relative to biadamantylidene **1** vs. the calculated $C(sp^3)C(sp^2)C(sp^3)$ bond angle of the neutral olefin.

is a significant through-bond component to the increase in oxidation potential for heteroatom substitution.

$E^{\circ\prime}$ data are now available for nine tetra-α-branched bisbicyclic monoolefins and are plotted along with the $E^{\circ\prime}$ for their acyclic analogue, tetraisopropylethylene (**16**), in Figure 8. The vertical axis shows the change in free energy for electron transfer relative to **1**,**1** in kcal/mol, and we have arbitrarily chosen the horizontal axis as the C(C=)C bond angle obtained from Allinger MM.2 calculations[30] on the neutral olefin. We chose this plot because binorbornylidene (**11**) is the most difficult compound to oxidize, and its bicyclic rings hold this angle to be the smallest in the series, but the bond angle effect is rather clearly not the reason for **11** being so hard to oxidize. We note the orbital symmetry argument first presented by Hoffmann and co-workers,[31] which we have discussed previously.[32] The 0.18 V easier adiabatic electron loss in solution for antisesquihomobicycloheptene **15** than its syn analogue **14** is only 0.9 kcal/mol smaller than the 0.22 eV difference in their gas phase vertical ionization potentials (7.90 and 8.12 eV, respectively),[33] which is probably within experimental error of being the same size. The reported vertical ionization potential for tetraisopropylethylene (**16**) is 8.13 eV, which is 0.29 eV higher than that of **1**,[34] also within experimental error of their 0.30 V difference in E°.

Mechanism of Olefin Cation Radical Oxygenation. There appear to be three propagation steps in the olefin cation radical oxygenation chain, as shown in Scheme V. The open peroxycarbenium cation B^+ has not yet been seen spectroscopically,[8] but its presence has been inferred from the products of oxygenation of **10**, which produces about 20% of the same dioxetane as that derived from **9**, which has the syn distribution of the alkyl groups, requiring rotation about the central CC bond.[10] It was shown

Scheme V

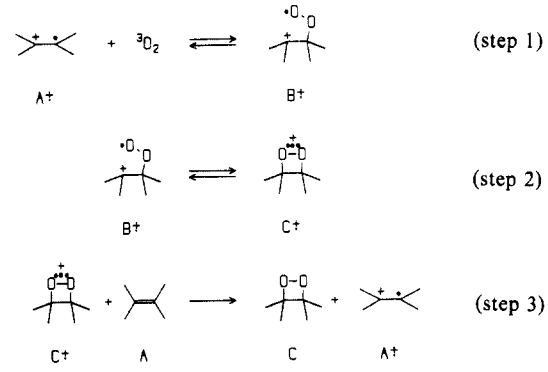

that the rotation is not occurring in the olefin cation radical (A^+ of Scheme V). If B^+ is present in significant concentration, it must not be electroactive between about +1.4 and 2 V vs. SCE, or a redox wave corresponding to it ought to have been seen. We suggest that it is reasonable that B^+ would not reduce in this region, and hence not be able to carry the oxygen addition chain by electron transfer. In Hückel terms, the resonance integral β between the two p orbitals of an olefin stabilizes its bonding orbital relative to that of an isolated p orbital substantially. In the gas phase, the ionization potential for $(CH_3)_3C^{\bullet} \rightarrow (CH_3)_3C^+$ is 6.92 eV,[35] about 1.5 eV lower than that of $Me_2C{=}CMe_2$. We doubt that the effect of a β peroxy substituent would be able to raise the B,B^+ ionization potential enough to overcome such a large difference. It is therefore not surprising that B^+ is observed to be electroinactive in the region where we can look for it, even if it is present in significant concentration, which is not actually known. Closure of B^+ to C^+ puts the "hole" in the π^* orbital of the OO bond. Peroxides have substantially higher IP values than olefins,[36] and their $E^{\circ\prime}$ values in solution are also higher.[8] Step 3 of Scheme V is exothermic by about 15.2 kcal/mol at −78 °C, the difference between the formal oxidation potentials of **1** and **2** under the same conditions. It is certainly not obvious that B^+ ever builds up in concentration. Experiments **9** and **10** establish that closure of B^+ is faster than CC bond rotation.[10] If the closure rate were slower than about 10^5 s^{-1} and B^+ were electroinactive, as suggested above, there would be substantial $[O_2]$ dependent effects on the voltammograms, but simulations including B^+ as an intermediate did not lead to an improved fit to the experimental data under any conditions, and it seems most likely that the closure rate is fast on the CV time scale.

Because we are presently unable to detect B^+, we cannot separate steps 1 and 2 of Scheme V in the CV experiments, but the results presented above lead to a significant conclusion. Comparing second-order with first-order reactions requires consideration of concentrations, and under the CV conditions of 7.5 mM O_2, the $k_{on}[O_2]$ value is 42 s^{-1} at room temperature, while k_{off} is at least 800 s^{-1}. This means that the $\mathbf{1}^+ + O_2 \leftrightarrow \mathbf{2}^+$ equilibrium is endothermic by at least 2 kcal/mol under these conditions. The overall addition reaction is only favorable because the very exothermic electron transfer of step 3 pulls the oxygen addition through an unfavorable prior equilibrium. We suggest that the large temperature effect on the chain length (about 10 for 1 at room temperature, but over 800 at −78 °C[7]) is primarily a result of $\mathbf{2}^+$ decomposing too rapidly at room temperature. One of the more interesting aspects of the olefin cation radical oxygenation is that simply allowing $\mathbf{1}^+$ to react with oxygen generates $^2/_3$ of an electron volt of oxidizing powder.

The oxygenation of **5**(Cl) gives 25 times as much of the product from addition of oxygen on the face of the olefin syn to the chlorine-bearing carbon as that from the opposite face (Scheme

(30) Allinger, N. L. *J. Am. Chem. Soc.* **1977**, *99*, 8127. Quantum Chemistry Program Exchange, No. 395, Indiana University Bloomington, Indiana.
(31) Hoffmann, R.; Mollere, P. O.; Heilbronner, F. *J. Am. Chem. Soc.* **1973**, *95*, 4860.
(32) Nelsen, S. F.; Kapp, D. L. *J. Org. Chem.* **1985**, *50*, 1339.
(33) Brown, R. S.; Buschek, J. M.; Kopecky, K. R.; Miller, A. J. *J. Org. Chem.* **1983**, *48*, 3692.
(34) Mollere, P. D.; Houk, K. N.; Bomse, D. S.; Morton, T. H. *J. Am. Chem. Soc.* **1976**, *98*, 4732.
(35) (a) By pes: Houle, F. A.; Beauchamp, J. L. *J. Am. Chem. Soc.* **1979**, *101*, 4067. (b) By electron impact: Lossing, F. B.; Semeluk, G. P. *Can. J. Chem.* **1970**, *48*, 955.
(36) For a discussion of substituent and angle effects on peroxide ionization potentials, see: Nelsen, S. F. *J. Org. Chem.* **1984**, *49*, 1891 and references therein.

IV), despite the similarity in steric effects for approach to the two faces. Even addition to the more favored syn face is only 40% as fast for $5(Cl)^+$ as for 1^+ (Table IV), so the disfavored anti attack must be less than 2% as fast. We were initially surprised by this result, because the chlorinated cation radical is over 5 kcal/mol destabilized compared to its neutral form, and we thought the less stable cation radical ought to be the more reactive one. Conversion of A^+ and B^+, however, is formally a nucleophilic attack of the remaining π electron on oxygen. The carbon bound to oxygen in the product is obviously oxidized, but so is the other carbon, which increases in formal charge density from $^1/_2$ to 1. It is understandable, then, that the electron-withdrawing chlorine atom slows attack to both faces but especially slows attack opposite the chlorine-bearing alkyl group, which would have the larger interaction at the pyramidalized transition state for addition in an anti attack. The selectivity in attack at **9**[10] and slower rate of oxygen addition (Table IV) compared to **1** are in agreement with this interpretation. Although steric effects could rationalize **9** adding oxygen faster from the side opposite the three carbon bridges, they could not predict the slowing of addition to **9** compared to **1** (addition in the latter is clearly more hindered) nor the approximately equal rates for oxygen addition to **9** and **10** (if steric effects were large enough to make only one product seen from **9**, one would surely predict a detectable difference in rate for **9** and **10**, where each face of the olefin has one $(CH_2)_3$ group).

Conclusion

Cation radical chain oxygenation of **1** to **2** involves a rather slow (k_2 = 5600 M^{-1} s^{-1} at room temperature), reversible addition of oxygen to 1^+, and the equilibrium between 1^+, $^3O_2$, and 2^+ is significantly endothermic. The addition is driven by the highly exothermic electron transfer from **1** to 2^+. Despite the rather slow oxygen addition, long chains are observed at −78 °C. Smaller alkyl groups than those of **1** substantially increase the rate of oxygen addition. For olefins with different π faces, the face selectivity for the radical cation chain reaction is higher than for $^1O_2$ addition but in the same direction; oxygen addition from the side opposite the best cation-stabilizing alkyl groups is favored. When amounts of steric hindrance to oxygen addition are similar, the cation radical with poorer cation-stabilizing alkyl groups (the olefin with the higher $E°'$ value) reacts more slowly with oxygen.

Experimental Section

Materials. We thank Prof. H. Prinzbach and L. and I. Knothe (Freiburg) for providing **11**, Prof. E. L. Clennan (Wyoming) for **17**, and Prof. S. J. Cristol (Colorado) for **18**. The samples of **5**(Cl) and **7**(Cl_2) used were prepared by the method of Kellog and co-workers,[14] **8** by the method of Schaap and Faler,[37] **14** by the method of Paquette and Carr,[38] **15** by the method of Bartlett and co-workers,[26] and **16** by that of Tidwell and Langler.[40] The preparations used for **9** and **10**,[10] generation of **13** in solution,[32] and of **19**[7] and **21**[8] appear elsewhere, and the preparation of **12**, the details of which were provided by Prof. Wynberg (Groningen), will be published elsewhere.

4(e)-Methoxyadamantylideneadamantane, 5(OMe). **5**(Cl) (0.6 g, 0.20 mmol) was dissolved in 30 mL of dry THF. Methanol (10 mL) and 0.35 g of silver nitrate (0.21 mmol) were added, and the solution was heated to reflux overnight. The solution was cooled, filtered, and partitioned between diethyl ether and water. The organic layer was extracted with water, dried with potassium carbonate, and evaporated to yield a white solid which was purified via preparative liquid chromatography to give 150 mg (0.5 mmol, 25%) **5**(OMe), mp 68–69 °C [^{1}H NMR ($CDCl_3$) δ 3.30 (s, 3 H), 3.2–2.8 (m, 5 H), 2.3–1.2 (m, 22 H); IR ($CDCl_3$) 2900, 1450, 1270 cm^{-1}. MS, M^+ = 298 as base peak]. (The methoxide could also be prepared by methylation of **5**(OH) with methyl lithium/methyl iodide.) The major fraction (330 mg, 50%) in the solvolysis was determined to be the nitrate ester of 4(e)-hydroxyadamantylideneadamantane, **5**(ONO_2): ^{1}H NMR ($CDCl_3$) δ 4.90 (br s, 1 H), 3.15 (br s, 1 H), 2.90 (br s, 3 H), 2.2–1.5 (m, 22 H); IR 2900, 2850, 1630, 1450, 1280 cm^{-1}; MS, (rel intensity) M^+ = 329 (10), 283 (100), 267 (70).

4(e)-Hydroxyadamantylideneadamantane Trifluoroacetate, 5-(O_2CCF_3). A mixture of 0.1 g of **5**(Cl) (0.3 mmol), 10 mL of methylene chloride, 0.5 mL of trifluoroacetic acid, and 0.5 mL of trifluoroacetic anhydride was stirred 30 min at room temperature. The reaction was quenched by the addition of water; the organic layer was washed with water and then saturated sodium carbonate solution. The solution was dried with potassium carbonate and evaporated to give 90 mg (0.24 mmol, 71%) of the trifluoroacetate as a clear oil: ^{1}H NMR ($CDCl_3$) δ 4.95 (br s, 1 H), 3.15 (br s, 1 H), 2.85 (br s, 3 H), 2.2–1.4 (m, 22 H); IR 2920, 2850, 1780, 1450, 1220, 1160 cm^{-1}; MS, M^+ = 380 as 80% of base peak (69).

5-Methoxyadamantylideneadamantane, 6(OMe). To a solution of 2-adamantyl iodide (354 mg, 1.35 mmol) in diethyl ether at −43 °C (acetonitrile slush) was added 1.4 mL of 1.9 M *tert*-butyllithium in pentane.[39] The solution was stirred for 30 min, and then a solution of 240 mg (1.33 mmol) of 5-methoxyadamantanone in 2 mL of diethyl ether was added. The solution was warmed to room temperature, washed with water and saturated bicarbonate, and dried with magnesium sulfate to give a white semisolid. The crude alcohol was purified by preparative LC, dissolved in 5 mL of freshly distilled Me_2SO, and heated to 170 °C for 4 h. The solution was cooled to room temperature and partitioned between pentane and water. The organic solution was washed with water and saturated sodium bicarbonate solution and dried with magnesium sulfate. Evaporation of solvent and sublimation yielded a sample of 5-methoxyadamantylideneadamantane (approximately 20 mg), mp 68–69 °C, which was used without further purification: ^{1}H NMR ($CDCl_3$) δ 3.23 (s, 3 H), 3.12 (br s, 2 H), 2.90 (br s, 2 H), 2.0–1.6 (m, 19 H).

4(e)-Chloroadamantanone. The procedure followed is a modification of the procedure used in the synthesis of 4(e)-bromoadamantanone.[42] A mixture of 4 g (27 mmol) of adamantanone, 1.86 g (27 mmol) of hydroxylamine hydrochloride, and 50 mL of concentrated hydrochloric acid was slowly heated to 100 °C. After heating for 24 h, the solution was cooled and poured into saturated sodium bicarbonate solution. The aqueous layers were extracted with diethyl ether, which was extracted with saturated sodium bicarbonate solution. The organic layer was dried with potassium carbonate and evaporated to give a white solid. Purification of half of the crude ketone by sublimation and preparative LC gave 950 mg (5.2 mmol, 20%) 4(e)-chloroadamantanone, mp 210–212 °C: ^{1}H NMR ($CDCl_3$) δ 4.30 (br s, 1 H), 2.76 (br s, 1 H), 2.7–2.4 (m, 3 H), 2.3–1.7 (m, 8 H); IR 2920, 2860, 1730, 1460 cm^{-1}; MS, M^+ = 184 as 25% of base peak at *m/e* 121.

2-Isopropylidene-4(e)-chloroadamantane, 20. 4(e)-Chloroadamantanone (600 mg, 3.25 mmol) was dissolved in 50 mL of THF. The solution was cooled to −78 °C, and 10 mL of a 0.36 M solution of isopropyllithium in pentane was added. The solution was stirred 4 min at −78 °C and then quenched by addition of 2 mL of methanol. The reaction mixture was warmed to room temperature, diluted with diethyl ether, and extracted first with water and then saturated sodium carbonate solution. Drying with potassium carbonate and evaporation of solvent gave 680 mg of a mixture of approximately 7:1 of isomeric alcohols [^{1}H NMR ($CDCl_3$) δ α-chloro proton major 4.41 (br s, 1 H), minor 4.87 (br s, 1 H), 2.2–1.5 (m, 13 H), 0.89 (m, 6 H)]. Addition of increments of $Eu(fod)_3$ of a solution of alcohols in $CDCl_3$ resulted in a slightly greater shift for the minor isomer (ppm/0.25 equiv $Eu(fod)_3$ = 0.254 (major), 0.378 (minor)).

The mixture of alcohols was dissolved in 20 mL of methylene chloride. In succession were slowly added 10 mL of triethylamine, 4 mL of methanesulfonyl chloride, and 20 mL of methylene chloride. The solution was heated to reflux for 2 days and then stirred at room temperature for 5 days. Water and methylene chloride were added, and the layers were separated; the organic layer was washed with saturated sodium bicarbonate and dried with potassium carbonate. Evaporation of the solvent gave an oil which solidified upon bulb-to-bulb distillation to 270 mg of **20** as a pale yellow solid, mp 48–50 °C (40%): ^{1}H NMR ($CDCl_3$) δ 4.25 (br s, 1 H), 3.00 (br s, 1 H), 2.80 (br s, 1 H), 2.35 (tm, 2 H), 2.1–1.4 (m, 8 H), 1.65 (s, 6 H); IR 2910, 2850, 1450 cm^{-1}; MS, M^+ 210 as 20% of base peak at *m/e* 69.

Chemical Shift Assignments for 22 and 23. Isomer **22** has a *CH*Cl proton shift δ' of 4.50 δ and **23**, 4.42. The major isomer **26** obtained upon borohydride reduction of **24** (2.5 parts) has δ' = 4.20, and the minor product **25**, δ' = 4.75, which was shown to be the correct assignment by pseudo contact shifts.[26] In agreement with this result of larger δ' when OH is syn to the chlorine-bearing carbon, isopropyllithium addition to **24** generated 6 parts of **28** (δ' 4.41) to one part of **27** (δ' 4.78), and a slightly larger pseudo contract shift was observed for **27** than for **28**. No differential pseudo contact shift was observed for **22** and **23**, but the

(37) Schaap, A. P.; Faler, G. R. *J. Org. Chem.* **1973**, *38*, 3061.
(38) Paquette, L. A.; Carr, R. V. C. *J. Am. Chem. Soc.* **1982**, *104*, 7553.
(39) Wieringa, J. H.; Wynberg, H. *Synth. Commun.* **1971**, *1*, 7.
(40) Langler, R. F.; Tidwell, T. T. *Tetrahedron Lett.* **1975**, 777.
(41) Bomse, D. S.; Morton, T. H. *Tetrahedron Lett.* **1975**, 781.
(42) Vodicka, L.; Triska, J.; Hajeck, M. *Collect. Czeck. Chem. Commun.* **1980**, *45*, 2670.

assignment shown based on chemical shifts is reasonable and also agrees with that of Wynberg and co-workers.[27]

Cyclic Voltammetry. The electrochemical instrumentation and procedures for resistance compensation were the same as described previously.[43] The digital data acquisition system was used for most of the voltammograms which were to be compared with simulations though some were recorded with a Houston "omnigraphic" X-Y recorder (<0.5 V/s) or Tektronix 5000 storage oscilloscope (>0.5 V/s) followed by digitization of the data. The background-corrected voltammograms were smoothed[44] and compared with the simulations.[21]

A standard three electrode cell was used. Nitrogen, air, or oxygen was admitted through a needle in a septum and expelled through a mineral oil bubbler. The working electrode was a platinum disk sealed in soft glass. It was polished with 5.0 and 0.3 micron alumina on a polishing cloth between voltammograms. The counter electrode was a coiled 1-in. length of platinum wire. The reference electrode was a Corning ceramic junction SCE which was placed in a compartment separated from the test solution by a cracked glass bead. Temperature control was by way of an external cooling bath, typically dry ice/acetone. The cell was equipped with a small Teflon-coated stirring bar, and the sample was stirred between scans. The special procedures needed to obtain electrochemical data with methylene chloride solvent and with methylene chloride/trifluoroacetic anhydride/trifluoroacetic acid solvent both at room temperature and at -78 °C are fully described elsewhere.[21]

(43) O'Connell, K. M.; Evans, D. H. *J. Am. Chem. Soc.* **1983**, *105*, 1473.
(44) Fitch, A.; Evans, D. H. *J. Electroanal. Chem.*, in press.

Acknowledgment. We thank the Petroleum Research Fund, administered by the American Chemical Society, and the National Science Foundation for partial financial support of this work and the Amoco Oil Company and the Wisconsin Alumni Research Foundation for fellowships to D.L.K. We thank Mark F. Teasley for the CV work on **14** and **15**.

Registry No. 1, 30541-56-1; **1**$^{+\cdot}$, 70535-07-8; **2**, 35544-39-9; **5** (OMe), 89543-36-2; **5** (Cl), 79732-69-7; **5** (Cl)$^{+\cdot}$, 104418-84-0; **5** (O_2CCF_3), 104335-93-5; **6** (OMe), 104335-94-6; **7**, 77331-40-9; **7**$^{+\cdot}$, 104418-85-1; **8**, 55993-21-0; **9**, 100208-23-9; **9**$^{+\cdot}$, 100296-10-4; **10**, 100208-24-0; **10**$^{+\cdot}$, 100296-11-5; **11**, 51689-29-3; **12**, 30614-34-7; **13**, 88656-03-5; **14**, 73321-28-5; **15**, 73679-39-7; **16**, 7090-88-2; **17**, 65498-90-0; **18**, 29309-28-2; **19**, 20441-18-3; **20**, 104335-95-7; **21**, 99810-86-3; **22**, 104335-96-8.

^{1}H NMR Probes of the Binuclear Iron Cluster in Hemerythrin

Michael J. Maroney,[†§] Donald M. Kurtz, Jr.,*[‡] Judith M. Nocek,[‡] Linda L. Pearce,[‡] and Lawrence Que, Jr.*[†]

Contribution from the Departments of Chemistry at the University of Minnesota, Minneapolis, Minnesota 55455, and Iowa State University, Ames, Iowa 50010. *Received April 14, 1986*

Abstract: ^{1}H NMR spectroscopy has been used to probe the various redox states of hemerythrin (Hr) to gain insight into the structural and magnetic changes that may occur in these states. In all, three oxidation states have been studied: deoxy [Fe(II),Fe(II)], semimet [Fe(II),Fe(III)], and met and oxy [Fe(III),Fe(III)]. The solvent-exchangeable imidazole NH protons of histidine ligands to the metal centers can be observed in all these complexes. For the met and oxy forms of the protein, these protons are found near 20 ppm, a shift significantly decreased from that found in mononuclear high-spin ferric imidazole complexes (ca. 100 ppm). This decrease in shift is consistent with the strong antiferromagnetic coupling ($J = -100$ cm^{-1}) found for these complexes. For the deoxyHr complexes, the NH shifts range from 40 to 80 ppm, values comparable to those found for mononuclear high-spin ferrous complexes. This result shows the iron centers in the deoxy forms are not strongly coupled. Evans' susceptibility measurements on deoxyHr and deoxyHrX (X = N_3^-, NCO^-, F^-) show the presence of a weak antiferromagnetic interaction ($J = -15$ cm^{-1}) in deoxyHr and even weaker interactions in deoxyHrX ($J = -11, -5, 0$ cm^{-1} for X = F^-, NCO^-, N_3^-, respectively). For the semimetHr complexes, the NH shifts are also indicative of weak coupling. In all complexes except μ-SsemimetHr, J is estimated to be ca. -20 cm^{-1} from the temperature dependences of the shifts of the Fe(III)-coordinated imidazole NH's. The NMR spectra also show that the iron atoms have a trapped valence formulation on the NMR time scale, with the anion coordinated to the ferric center. The small J values found for the deoxyHr and semimetHr complexes are consistent with the J values found for synthetic Fe(III)-Fe(III) and Fe(II)-Fe(II) complexes with μ-hydroxo-di-μ-acetato bridging units and suggest that the oxo bridge found in the met and oxy forms of hemerythrin has become protonated upon reduction. The persistence of a bridge between the metal centers in the various states of hemerythrin would facilitate the electron transfer required for reversible oxygenation. The NMR data support the mechanism proposed by Stenkamp et al. (*Proc. Natl. Acad. Sci. U.S.A.* **1985**, *82*, 713-716) for reversible oxygenation wherein the proton on the hydroxo bridge of deoxyHr is transferred to the bound peroxide as deoxyHr is converted to oxyHr. The stability of the semimetHrX complexes suggests that semimetHr superoxide [Fe(II),Fe(III) O_2^-] is a reasonable transition state in the oxygenation process.

Hemerythrin (Hr), a respiratory protein isolated from a number of marine invertebrates, contains a binuclear non-heme iron oxygen-binding site.[1] The structures of the iron clusters in oxyHr, metHr, and metHrN_3, where both iron atoms are high-spin ferric centers, have been well-characterized by X-ray crystallographic studies[2-4] and have recently been modelled by synthetic complexes.[5,6] The structure of metHr that emerges from these studies and physical studies of the active site[7-16] (**1**) has one five-coordinate iron atom (Fe_a) and one six-coordinate iron atom (Fe_b). The two

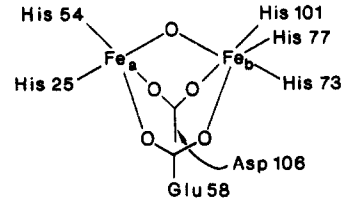

iron atoms are bridged by two carboxylate ligands, one each from glutamate and aspartate residues, and an oxo group. The presence

[†] University of Minnesota.
[‡] Iowa State University.
[§] Present address: Department of Chemistry, University of Massachusetts, Amherst, MA 01003.

(1) Klotz, I. M.; Kurtz, D. M., Jr. *Acc. Chem. Res.* **1984**, *17*, 16-22. Sanders-Loehr, J.; Loehr, T. M. *Adv. Inorg. Biochem.* **1979**, *1*, 235-252.

0002-7863/86/1508-6871$01.50/0 © 1986 American Chemical Society